

CFHT AO Imaging of the CLASS Gravitational Lens System B1359+154

D. Rusin¹, P.B. Hall^{2,3}, R.C. Nichol⁴, D.R. Marlow¹, A.M.S. Richards⁵

and

S.T. Myers^{1,6}

ABSTRACT

We present adaptive optics imaging of the CLASS gravitational lens system B1359+154 obtained with the Canada-France-Hawaii Telescope (CFHT) in the infrared K band. The observations show at least three brightness peaks within the ring of lensed images, which we identify as emission from multiple lensing galaxies. The results confirm the suspected compound nature of the lens, as deduced from preliminary mass modeling. The detection of several additional nearby galaxies suggests that B1359+154 is lensed by the compact core of a small galaxy group. We attempted to produce an updated lens model based on the CFHT observations and new 5-GHz radio data obtained with the MERLIN array, but there are too few constraints to construct a realistic model at this time. The uncertainties inherent with modeling compound lenses make B1359+154 a challenging target for Hubble constant determination through the measurement of differential time delays. However, time delays will offer additional constraints to help pin down the mass model. This lens system therefore presents a unique opportunity to directly measure the mass distribution of a galaxy group at intermediate redshift.

Subject headings: gravitational lensing

¹Department of Physics and Astronomy, University of Pennsylvania, 209 S. 33rd St., Philadelphia, PA 19104-6396, USA

²Department of Astronomy, University of Toronto, 60 St. George Street, Toronto, ON M5S 3H8, Canada

³Visiting Astronomer, Canada-France-Hawaii Telescope, operated by the National Research Council of Canada, the Centre National de la Recherche Scientifique de France and the University of Hawaii

⁴Department of Physics, Carnegie Mellon University, 5000 Forbes Ave., Pittsburgh, PA 15232

⁵NRAL, Jodrell Bank, University of Manchester, UK

⁶current address: National Radio Astronomy Observatory, Socorro, NM, USA

1. Introduction

The gravitational lens system CLASS B1359+154 (Myers et al. 1999) was discovered in the third phase of the Cosmic Lens All-Sky Survey (Myers et al. 2000), an international program that has imaged over 15,000 flat-spectrum radio sources at 8.5 GHz using the Very Large Array (VLA) in A-configuration. The survey seeks to find new cases of gravitational lensing for a variety of cosmological studies. B1359+154 was identified as a lens directly from its VLA snapshot map, which featured four compact radio components arranged in a configuration indicative of lensing. Subsequent optical observations of the system with the Keck II telescope yielded a redshift of $z = 3.235$ for the lensed background quasar. No spectral features due to the lensing object were identified. Preliminary mass modeling based on the positions and flux density ratios of the four lensed radio components strongly suggested that the lens would be compound, as single-deflector models provided extremely poor fits to the observables. The system was imaged with the Canada-France-Hawaii Telescope (CFHT) to investigate this claim.

In this letter we first summarize the radio data, including a new high resolution 5-GHz map obtained with the Multi-Element Radio-Linked Interferometer Network (MERLIN). We then present a CFHT infrared image of B1359+154, taken using adaptive optics, which conclusively demonstrates that the lensing mass is distributed among multiple galaxies. Next, new mass models based on the above observations are explored. We conclude by discussing the implications of the CFHT data, along with suggestions for future studies of this very interesting lens system.

2. Radio Properties

CLASS B1359+154 was discovered during the CLASS-3 observations of March 1998. Its VLA survey snapshot map showed four compact components (A–D) arranged in a configuration indicative of a quadruply-imaged source, plus a fifth extended component inside the four-image configuration. A deep VLA follow-up observation at 8.5 GHz resolved the fifth component into a pair of sub-components (E and F). Subsequent VLA observations at 15 GHz were performed to study the spectral properties of the system. The spectral index of component E between 8.5 and 15 GHz ($\alpha_{8.5}^{15} \approx -0.6 \pm 0.2$, where $S \propto \nu^\alpha$) was found to be flatter than that of the outer four components ($\alpha_{8.5}^{15} \approx -0.9 \pm 0.1$). This suggested that E was not an additional lensed image, but rather emission from a weak AGN associated with one of the lensing galaxies. Component F was not detected at 15 GHz. The upper limit placed on its spectral index ($\alpha_{8.5}^{15} < -0.6$) could not rule out the possibility of it being a fifth lensed image.

MERLIN 5-GHz observations of B1359+154 were performed 1999 January 26 and February 6. The two observations gave a total integration time of 24 hr on-source. The combined data set was calibrated in AIPS and subsequently imaged and modelfitted with Gaussian components in DIFMAP (Shepherd 1997). The final map is displayed in Fig. 1 and has a 60 mas beam size. The RMS noise level in the map is 40 μ Jy/beam. The map shows all six radio components previously

detected with the VLA. Each component was modeled by a single compact Gaussian. There were hints of a very weak flux bridge joining E and F at the 2σ level in the residual map. Table 1 lists the component positions, flux densities and spectral indices between 5 and 8.5 GHz. We estimate the uncertainties in the spectral indices to be 0.2 for A–E and 0.5 for F. Therefore we cannot dismiss the possibility that component F is an additional lensed image based on its radio spectrum. Interestingly, component D appears to have a flatter spectrum between 5 and 8.5 GHz than A–C. This discrepancy may be due to component variability. To test this assumption, we reduced each of the two MERLIN data sets separately. We found tentative evidence for variability in the lensed components at the 10% level.

It should be noted that the distribution of flux densities among the B1359+154 lensed radio components is quite peculiar. Based on studies of isolated lens galaxies, we would expect one of the merging images (B and C) to be the most highly magnified. However, component A is consistently brighter than B or C in our radio maps.

3. CFHT Observations

Infrared observations of B1359+154 using the CFHT were performed 1999 June 23–25. Because of its close proximity to a bright star, the system was investigated using the Adaptive Optics Bonnette (known as *Pue'o*; Rigaut et al. 1998) with the KIR camera, a 1024×1024 Hg:Cd:Te detector with platescale $0\farcs0348/\text{pixel}$. All observations were made with the K' filter (centered at $2.120 \mu\text{m}$ with a FWHM of $0.340 \mu\text{m}$) using full AO correction. Exposures were 5 minutes long, taken in a repeated 9-position dither pattern. Images were flat-fielded using the difference between dome flats taken with lamps on and off. Each night's flat-fielded data set was medianed to form a blank sky image which was then subtracted. Integer-pixel image shifts were determined using the guidestar and one other star visible on most images. An object mask image was produced from an initial coadd and a second-pass sky image was constructed with objects masked out. The final image consists of 3.25 hr of exposure coadded without pixel rejection.

A $4'' \times 4''$ section of the CFHT image, centered on the B1359+154 lens system, is displayed in Fig. 2. Infrared counterparts to all four lensed images are clearly detected. In addition, a region of extended emission is observed inside the ring of images, containing three distinct brightness peaks (K1–K3). The complexity of this extended emission is suggestive of multiple, superimposed lens galaxies. Overlaying the CFHT image with the MERLIN map, we see that component E is coincident with a weaker emission feature located between K1, K2 and K3. Component F is not associated with any of the observed brightness centers. A wide-field view ($18'' \times 18''$) of the system is displayed in Fig. 3. Several additional galaxies (K4 – K6) are observed within 10 arcsec of B1359+154. Traces of an infrared arc connecting components A, B and C are also visible in the image.

The CFHT data for B1359+154 are described in Table 1. Because components A, B, C and

K1–K6 have well-defined peaks, their positions may be approximated by eye from the pixel counts. We estimate an error of two pixels, or 70 mas, on these positions. The CFHT and MERLIN positions of images A, B and C are consistent within the observational uncertainties. Radio components D and E are also identified with CFHT emission features. However, these features are rather weak and irregular, and we did not attempt to estimate their positions.

NICMOS standards (Persson et al. 1998) measured in 20" diameter apertures were used to find a photometric solution to the K system, with 0^m037 RMS accuracy. The integrated magnitude of the B1359+154 lens system is $m_K = 17^m7$. Magnitudes for the individual CFHT emission features are given in Table 1. For A–C and K1–K3, magnitudes were calculated within a 0^{''}4 diameter aperture centered on the position of the CFHT emission peak. Identical apertures were also centered at the positions of radio components D and E. Because of the presence of significant amounts of extended emission, as well as the apparent superposition of many of the components, the derived magnitudes are particularly sensitive to the chosen aperture size. This problem does not affect K4–K6, which are well isolated from other emission features. Their magnitudes were therefore calculated with larger (1^{''}6 diameter) apertures, and sky-subtracted using an annulus located 1^{''}2 – 2^{''}0 from the objects.

4. Lens Modeling

Preliminary mass modeling results presented in Myers et al. (1999) strongly suggested that multiple deflectors were necessary to account for the B1359+154 radio data. Models consisting of a singular isothermal ellipsoid (SIE; Kormann et al. 1994) or an SIE plus external shear resulted in extremely poor fits ($\chi^2/\text{NDF} \gg 1000$ and $\chi^2/\text{NDF} > 10$, respectively), even after allowing for a large uncertainty of 20% on the image flux density ratios. An adequate fit was achieved by introducing a second deflector, parametrized as a singular isothermal sphere (SIS). The CFHT data has therefore validated the predication of a compound deflector system.

Constructing an improved mass model from the CFHT observations is difficult since it is impossible to be sure how many distinct galaxies reside within the Einstein ring. For example, one of the brightness peaks may be a star-forming region or disk disturbed by interactions rather than a galaxy center. Simply fixing deflectors to each of the emission peaks is therefore premature. On the other hand, because there are merely 11 constraints (8 positional coordinates and 3 flux density ratios) supplied by the MERLIN data, only relatively simple compound lens models can be explored if the positions of the deflectors are left as free parameters.

Though more and better constraints are needed to properly model this system, we tested a variety of plausible modeling scenarios based on the locations of the CFHT brightness peaks and the MERLIN radio data. We allowed for generous uncertainties of 5 mas on the positions and 20% on the flux density ratios of the lensed radio components, and assumed a lens redshift of $z_l = 1$.

We first attempted to update the SIE+SIS model by forcing each deflector to reside within

the Einstein ring, without actually fixing their centers to any observed emission peak. While this model fits the radio data well, it predicts a fifth lensed image that is significantly above the 3σ detection limit of the MERLIN map. The model must be discarded as this image is not observed. More complex models can be explored by fixing some subset of the deflectors to the infrared brightness centers (K1–K3, E). We investigated a series of two-SIE models in which one of the deflectors was fixed while the other was allowed to float. Each of the four attempts produced poor fits ($\chi^2/\text{NDF} \gg 100$). To study the possibility that more than two galaxies are present, we tested models consisting of two SIEs and one SIS, each fixed to a brightness peak. This is the most complicated model that can be constrained given the radio data. Distributing the deflectors among the four brightness peaks leads to 12 permutations of this model, all of which failed to produce a sufficient fit using reasonable parameters.

These attempts suggest that B1359+154 will be one of the most challenging gravitational lens systems to model. The acquisition of additional constraints is essential. Most importantly, we must determine how many galaxies are contributing to the lensing potential and pin down their precise locations. Additional constraints may also be obtained from the images, such as correlated milliarcsecond substructure in the lensed radio components and the ratios of measured time delays.

5. Conclusions and Future Work

CFHT AO observations of the CLASS gravitational lens system B1359+154 have detected infrared counterparts to each of the lensed radio components, as well as a region of extended emission within the four-image configuration. This region includes at least three distinct brightness centers, indicative of multiple, superimposed lensing galaxies. Several additional galaxies are observed to be flanking the system. As only 1.1 ± 0.3 galaxies would be expected down to $K = 21$ per $18'' \times 18''$ field (Hall, Green and Cohen 1998), this represents a significant overdensity. These observations suggest that the lensing mass in the B1359+154 system corresponds to the compact core of a small galaxy group.

The morphology of the K1–K3 emission region, along with the extremely poor fits provided by single-galaxy lens models, provide compelling evidence for a compound lens. The detection of coincident radio emission is consistent with this hypothesis, as AGNs are often triggered by interactions in dense environments. Interestingly, if there are more than two galaxies within the Einstein ring, they would each need to be significantly undermassive to produce an image splitting of only 1.7 arcsec. The lens candidate HST 180746+45599 (Ratnatunga, Griffiths and Ostrander 1999) also appears to be lensed by a small group of undermassive galaxies, possibly signaling the importance of such deflectors in arcsecond-scale lensing.

The confirmation of another compound lens system in CLASS seems to contradict the claim that lenses comprised of more than one primary galaxy should contribute negligibly to the overall lensing rate (Keeton, Kochanek and Seljak 1997). Three of the eleven new gravitational lens

systems discovered in CLASS – B1359+154, B1127+385 (Koopmans et al. 1999) and B1608+656 (Koopmans and Fassnacht 1999) – contain multiple galaxies within the Einstein ring. The lensing potentials of two additional systems – B1600+434 (Koopmans, De Bruyn and Jackson 1998) and B2319+051 (Marlow et al. 1999) – are strongly influenced by large secondary deflectors within a few arcseconds. Such observations suggest that compound deflectors play a significant role in lensing, a role that should be investigated with regard to lensing statistics analyses and constraints on the cosmological parameters.

Deep optical and/or near-infrared observations are needed to properly study the structure of the B1359+154 deflector system, pin down the number and positions of all galaxies present, and provide the necessary constraints on the mass model. High sensitivity, multi-color imaging with HST or Gemini is essential to correctly identifying all of the emission features, distinguishing among galaxy centers, star-forming regions and any disturbed disks or tidal tails which may have been induced by interactions. Because spectroscopy on each of the individual components is quite challenging, these observations will also provide vital photometric redshifts for the system. We should note that for a source at $z = 3.235$, the lens redshift is mostly likely to be $z \approx 0.7$ and may be as high as $z \approx 1$. The magnitude of the isolated galaxy K4 is consistent with an L^* elliptical in this redshift range for a flat Λ -dominated cosmology.

Much is still to be learned from high resolution radio investigations of this system. The detection of correlated milliarcsecond substructure in the lensed images would provide essential constraints to the mass model. As many as three additional constraints can be obtained from the ratios of measured time delays. The nature of radio component F also remains to be determined. At this time we cannot rigorously rule out the possibility of it being a fifth lensed image. If there are mass distributions centered at K1 and K3, the Fermat potential (Schneider, Ehlers and Falco 1992) should have a saddle point between them in which an image could form. Component F is located in this general region. Evidence for a faint flux bridge connecting E and F argues against the fifth-image hypothesis. A deep 1.7 GHz observation with the VLBA offers the best chance of conclusively detecting this flux bridge, if it exists.

B1359+154 has one of the most complex deflectors of any small separation (1–2 arcsec) gravitational lens system, and will be one of the most challenging lenses to model. Many more observational constraints are needed in order to meet this challenge. The construction of a viable mass model will offer a unique opportunity to probe the mass distribution of a small galaxy group at intermediate redshift. With the uncertainties inherent in the modeling of compound lenses, however, B1359+154 is unlikely to be a promising target for Hubble constant determination.

We thank the staff of the CFHT and MERLIN for their assistance during our observing runs. MERLIN is a national UK facility operated by the University of Manchester on behalf of PPARC. STM was supported by an Alfred R. Sloan Fellowship at the University of Pennsylvania. DR thanks Leon Koopmans for his advice and suggestions during the preparation of this draft.

REFERENCES

Hall, P.B., Green, R.F., Cohen, M., 1998, *ApJS*, 119, 1

Keeton, C.R., Kochanek, C.S., Seljak, U., 1997, *ApJ*, 482, 604

Koopmans, L.V.E., De Bruyn, A.G., Jackson, N., 1998, *MNRAS*, 295, 534

Koopmans, L.V.E., et al. 1999, *MNRAS*, 303, 727

Koopmans, L.V.E., Fassnacht, C.D., 1999, *ApJ*, accepted (astro-ph/9907258)

Kormann, R., Schneider, P., Bartelmann, M., 1994, *AA*, 284, 285

Marlow, D.R., et al. 1999, *AJ*, submitted

Myers, S.T., et al. 1999, *AJ*, 117, 2565

Myers, S.T., et al. 2000, in preparation

Persson, S. E., Murphy, D. C., Krzeminski, W., Roth, M., Rieke, M.J., 1998, *AJ*, 116, 2475

Ratnatunga, K.U., Griffiths, R.E., Ostrander, E.J., 1999, *AJ*, 117, 2010

Rigaut, F., et al., 1998, *PASP*, 110, 152

Schneider, P., Ehlers, J., Falco, E.E., 1992, *Gravitational Lenses* (New York: Springer)

Shepherd, M.C., 1997, in *Astronomical Data Analysis Software and Systems IV*, eds. G. Hunt and H. E. Payne, (ASP Conference Series, v125) 77

Table 1: CLASS B1359+154: MERLIN Positions and Flux Densities; CFHT Positions and Magnitudes.

Comp	MERLIN Data				CFHT Data		
	OFFSET (E)	OFFSET (N)	S_C (mJy)	$\alpha_5^{8.5}$	OFFSET (E)	OFFSET (N)	m_K
A	$+0''.0000 \pm 0''.0001$	$+0''.0000 \pm 0''.0001$	19.0	-1.3	$+0''.00$	$+0''.00$	20^m8
B	$-0''.4915 \pm 0''.0002$	$-1''.2480 \pm 0''.0002$	11.2	-1.2	$-0''.52$	$-1''.25$	20^m8
C	$-0''.3137 \pm 0''.0002$	$-1''.6640 \pm 0''.0002$	15.8	-1.3	$-0''.38$	$-1''.64$	20^m7
D	$+0''.9571 \pm 0''.0008$	$-1''.3660 \pm 0''.0008$	3.2	-1.0	-	-	21^m2
E	$+0''.6072 \pm 0''.0005$	$-1''.1420 \pm 0''.0005$	4.7	-1.5	-	-	20^m7
F	$+0''.4120 \pm 0''.0020$	$-0''.9580 \pm 0''.0020$	1.2	-1.7	-	-	-
K1	-	-	-	-	$+0''.63$	$-0''.70$	20^m7
K2	-	-	-	-	$+0''.52$	$-1''.50$	20^m7
K3	-	-	-	-	$+0''.14$	$-0''.94$	20^m7
K4	-	-	-	-	$+3''.62$	$-1''.36$	19^m1
K5	-	-	-	-	$-1''.81$	$+1''.50$	21^m0
K6	-	-	-	-	$-6''.51$	$-6''.99$	21^m0

Note. — MERLIN positions are offset from RA 14 01 35.5564 and Dec +15 13 25.789 (J2000). The rms noise level is $40\mu\text{Jy}$. Spectral indices between 5 GHz and 8.5 GHz are computed using the deep X-band observation presented in Myers et al. (1999). Uncertainties in the MERLIN positions are estimated from the beam size (60 mas) divided by the signal-to-noise. We estimate the uncertainties in the CFHT positions to be approximately 70 mas.

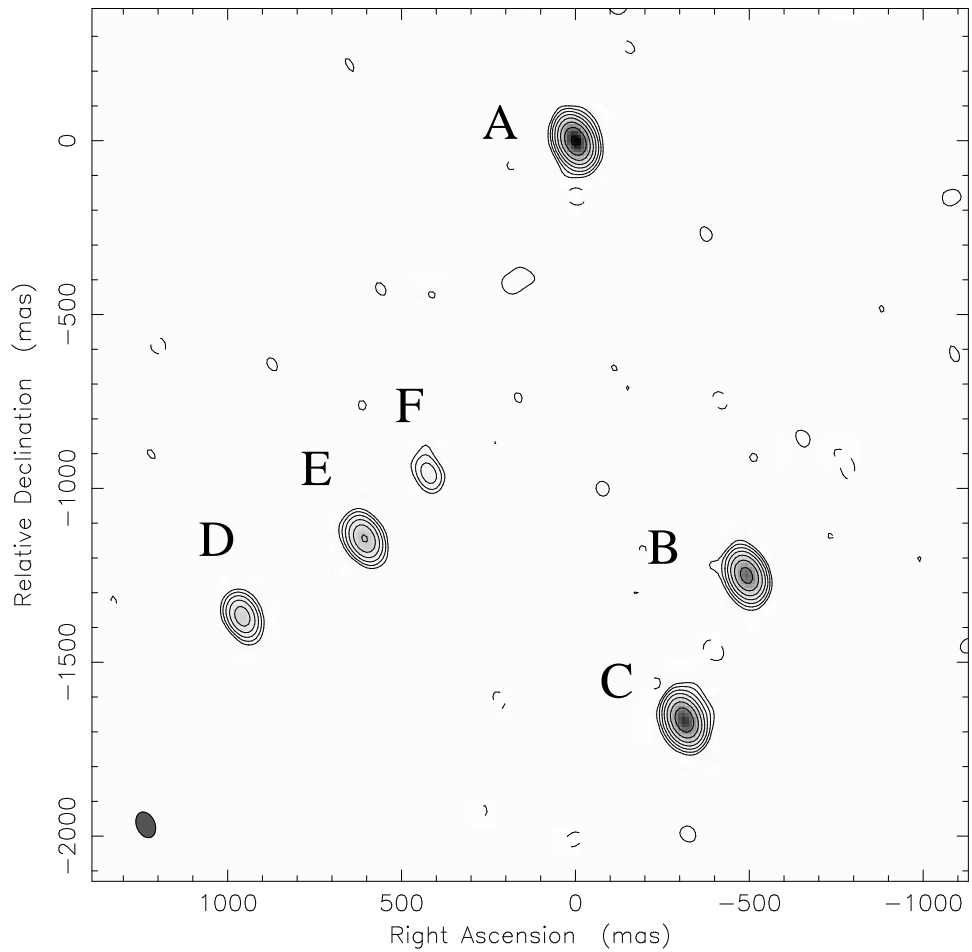


Fig. 1.— MERLIN 5-GHz map of B1359+154.

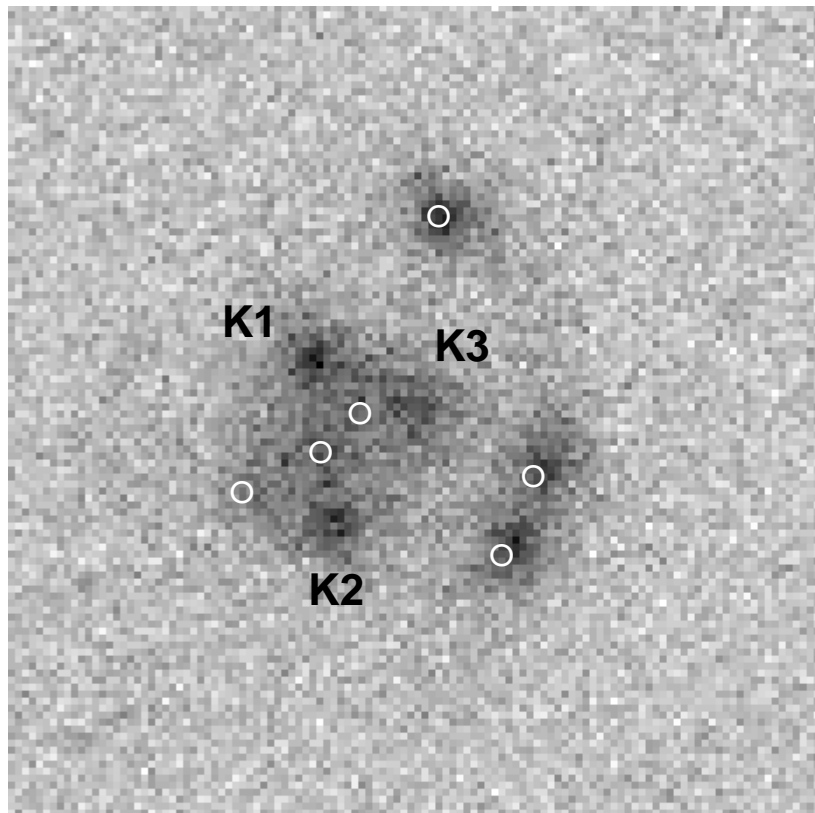


Fig. 2.— CFHT K-band image of B1359+154 ($4'' \times 4''$). Positions of the MERLIN radio components are denoted by circles. Radio component A is fixed to the peak of the corresponding CFHT emission feature.

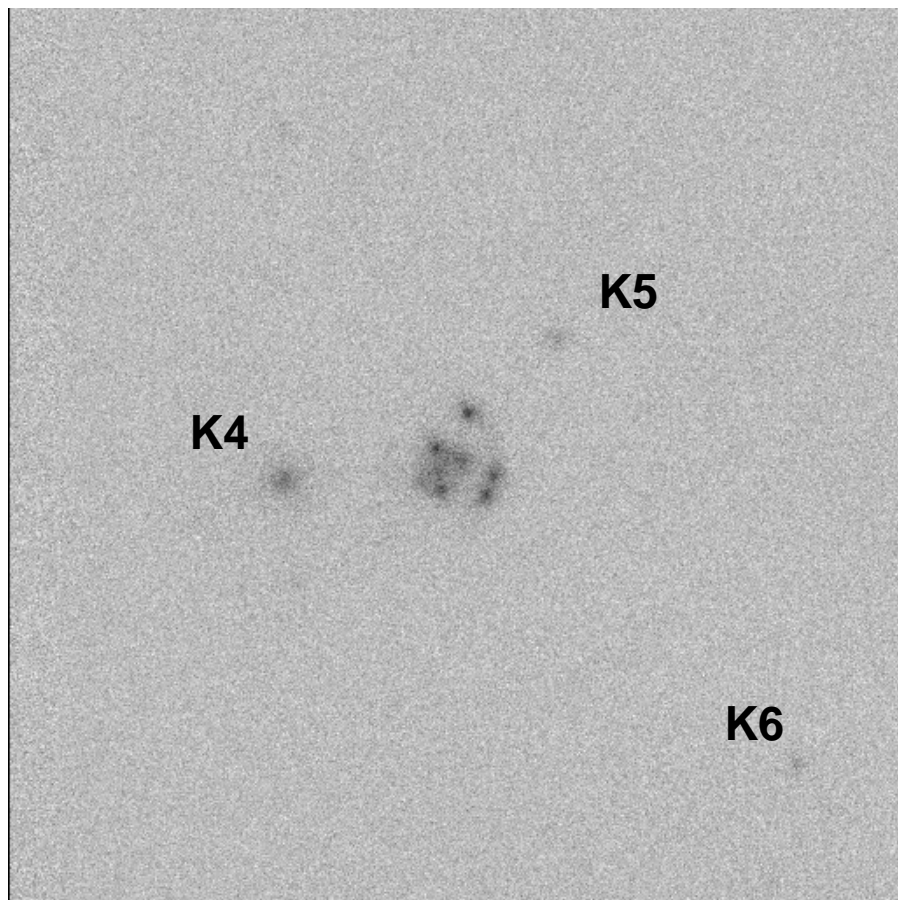


Fig. 3.— CFHT K-band image of B1359+154 ($18'' \times 18''$).